## A) Goal of the experiments

In literature, the effect of crystallization on the mechanical properties is still a matter of debate. Some researchers believe that a fraction of nano-crystallization in BMGs can help to increase their ductility, whereas others claim that crystallization dramatically decreases the fracture toughness. However, all agree on the importance of closely monitoring and controlling crystallization in order to achieve high mechanical properties. The goal of this study is to evaluate the effect of process parameters and scanning strategy on the occurrence of crystallization by combining in-situ monitoring during additive manufacturing and post-process scanning of the printed material. Another goal will be to measure accurately the critical time that it takes for crystals to nucleate after melting or heating by the laser beam.

# B) Background

Bulk Metallic Glass (BMG) is the name of a family of metallic alloys that do not have long-range order in their atomic structure, i.e., they are glassy, not crystalline. BMGs show enhanced properties, for instance, high hardness and strength, excellent corrosion and wear resistance, upper elastic limit, and low Young's modulus, owing to the disordered structure [1]. Due to the mentioned properties, they have attracted significant attention in different industries, such as electronics (as sensors and casing), jewelry, sporting goods and medical devices [1]. The processability of BMGs, which have been produced by conventional methods such as casting and melt spinning, is limited because of size restriction, poor machinability and lack of possibility of manufacturing samples with complex geometries without inducing crystallization [2-4]. Knowing how to overcome these restrictions can be a key to use BMGs for largescale applications. Selective Laser Melting (SLM) is a powder-bed additive manufacturing (AM) process that has gained a tremendous amount of attention among different industries and research groups in the last decade. In this method, a 3D CAD file is sliced into layers, and each layer is fused by selectively melting the powder using a laser beam [5, 6]. SLM has several advantages over conventional manufacturing methods, such as the possibility to build parts with complicated geometries and minimal feedstock waste. Since the interaction volume between the laser and deposited powder is small and the exposure time is short, the local cooling rate is very high (10<sup>3</sup>–10<sup>8</sup> K/s) which is typically higher than the critical cooling rate of most BMGs. Thus, it allows keeping the part in a glassy state and preventing crystallization. However, the cooling rate in the SLM process highly depends on the processing parameters [4]. Additionally, the layer-based nature of the process implies that a given location of the part undergoes several heating and cooling cycles when the laser beam melts subsequent layers. The formation of an amorphous-nanocrystalline composite during SLM is considered to be due to this reheating effect. Crystallization is highly probable to occur in the heat-affected zone (HAZ) where the temperature is higher than glass transition temperature but lower than melting temperature [7]. The effect of crystallization in BMGs on the mechanical properties has been investigated in the literature but remains a matter of debate. Although uncontrolled crystallization is highly detrimental to the mechanical properties, localized partial crystallization can be beneficial, by increasing ductility in an otherwise brittle material [8]. A better understanding of the effect of process parameters and scanning strategy on the crystallization process is thus required in order to be able to tailor the size, spatial distribution and volume fraction of crystalline inclusions.

A better understanding of the kinetics of crystallization during SLM is also essential. Ericsson et al. [8] recently developed a numerical model of the nucleation and growth of crystals from the supercooled liquid state. The model was calibrated using an

experimentally obtained TTT diagram of a Zr-based BMG (Zr<sub>59.3</sub>Cu<sub>28.8</sub>Al<sub>10.4</sub>Nb<sub>1.5</sub>). The crystallization at different temperatures was investigated using thermal analysis. Flash DSC was used to measure isothermal crystallization in the supercooled liquid region. However, this approach has several limitations. First, the DSC measurement conditions differ substantially from real SLM processing conditions. Second, the authors used the exothermic peak of crystallization as references to draw the TTT diagram (Figure 1), but the crystalline volume fraction at that moment is unknown. Finally, the critical time for nucleation measured by flash DSC is only obtained from cooling of the melt, whereas during SLM, most of the crystallization occurs during reheating, in the heat affected zone adjacent to the melt pool (Figure 2). High-speed *in situ* X-ray diffraction measurements offer solutions to these issues, together with the appropriate timescale resolution. It would allow us to determine in real processing conditions and with a high accuracy the onset of crystallization during both cooling of the melt pool and heating in the HAZ.

# C) Experimental method; specific requirements

Zr-based and Pd-based metallic glass powders with nominal compositions of Zr<sub>59.3</sub>Cu<sub>28.8</sub>Al<sub>10.4</sub>Nb<sub>1.5</sub> (at%) and Pd<sub>43</sub>Cu<sub>27</sub>Ni<sub>10</sub>P<sub>20</sub> (at%), respectively, are going to be 3D printed. SLM parameters (laser power, scanning speed, hatching distance, and layer thickness) have already been calibrated and are given in the following table:

	Power (W)	Scanning	Layer	Hatch	Spot size(µm)
		speed (mm/s)	thickness	distance (µm)	
			(µm)		
Zr-BMG	30-60	600	20, 30	50-75	30
Pd-BMG	50-150	600	40, 60	90-150	70

The in-situ and post-print scanning experiments will be performed with a miniaturized SLM device that is optimized for usage at synchrotron beamlines (Figure 3) [9, 10]. It consists of a scanning head with two mirrors to pilot the incoming laser beam onto the build stage, an objective-theta lens to focus the laser beam and a closed build chamber with windows for the X-ray beam entry and exit. The device was successfully implemented and tested at the MicroXAS and MS beamlines at SLS. We will work at 17.5keV, which results as a compromise between the need for sufficient transmission to probe bulk properties and sufficient flux for the high-speed measurements. Diffraction patterns will be recorded by the ultrafast 23 kHz EIGER detector positioned directly after the exit window of the SLM machine. Data reduction, analysis, and visualization will be performed with pyFAI and and in-house written Matlab routines.

#### D) Expected results

Preliminary test measurements were performed at the MS beam line on a 2×2×0.05 mm foil cut from a printed Zr-BMG sample. Figure 4 shows crystallization in the melt pool and in the HAZ in the same sample. Diffraction patterns were recorded at various positions of the foil and the presence of nanocrystals could be detected from small diffraction peaks superimposed with the broad peak of the amorphous matrix.

The following experiments will be performed during the present beamtime:

1) Studying the kinetics of crystallization during SLM. The time between when the laser passes and when crystallization occurs will be measured. As illustrated in Figure 2, crystallization mostly occurs in the HAZ, when the material is reheated to a temperature lower than its melting point. It also occurs, to a lower extent, after solidification of the melt pool. Both types of events will be studied. In order to clearly identify the occurrence of melting when the laser passes in the X-ray probe area, the powder will undergo a pre-SLM heat treatment so that it is partially crystallized rather

## Description (3/3)

than fully amorphous. The transition from partially crystallized powder to molten material will be easy to detect using high-speed X-ray diffraction.

- <u>2) Studying the effect of local heat accumulation on crystallization.</u> Figure 5 illustrates the locations where heat accumulates because of the changes in laser scanning direction. Since the heat input is higher in those locations, there is an increased probability for crystallization. We will study this effect by performing *in situ* experiments with the X-ray beam positioned near the edge and at the centre of the printed component and by using different scanning strategies (e.g. turn off the laser while switching to the next line).
- 3) Performing post-print spatially-resolved scanning to evaluate the effect of several thermal cycles on the solidified layers. During *in situ* monitoring, the X-ray beam cannot penetrate deep into the solidified material. Therefore, to control the effect of several thermal cycles on the solidified layers underneath, we will perfom post-print spatial resolved scanning as a function of depth. For that, we will build a thin wall of about 100 µm thickness. Line profiles will be recorded along the build direction in transmission mode. This should provide information on crystallization as a function of the distance from the top and side surface. Figure 6 demonstrates the feasibility of printing such thin wall specimen. It is a top view of a thin wall Zr-based BMG with a thickness of 110 µm and a height of 1 mm. We expect crystallization only in the solidified region where the temperature is higher than the glass transition temperature during laser processing, because the cooling rate in the melt pool is high enough to avoid crystallization.

With the help of *in situ* and post-print X-ray monitoring, we can optimize the laser process parameters such as to monitor the zones where crystals/nanocrystals are created, and to control their formation by adapting the process parameters.

# E) Estimate and justification of the beamtime

Based on previous in situ SLM experiments performed at MS we estimate we need about nine shifts of beam time. One day is dedicated to setting up the beamline, installing the SLM machine, aligning, implementing the synchronization and performing calibration measurements. The remaining 6 shifts are dedicated to the study of two BMGs with different chemical composition.

#### F) References relevant to the experiment description

- [1] J.F. Löffler, A. Andreas, A. Kündig, F.H.D. Torre, Rapid Solidification and Bulk Metallic Glasses Processing and Properties, in: Materials Process. Handb., Taylor& Francis Group, New York, 2007. [2] J. Schroers, Processing of Bulk Metallic Glass, Adv. Mater. 22 (2010) 1566–1597.
- [3] S. Pauly, L. Löber, R. Petters, M. Stoica, S. Scudino, U. Kühn, J. Eckert, Processing metallic glasses by selective laser melting, Mater. Today. 16 (2013) 37–41.
- [4] D.D. Gu, W. Meiners, K. Wissenbach, R. Poprawe, Laser additive manufacturing of metallic components: materials, processes and mechanisms, Int. Mater. Rev. 57 (2012) 133–164.
- [5] L.-C. Zhang, H. Attar, Selective Laser Melting of Titanium Alloys and Titanium Matrix Composites for Biomedical Applications: A Review, Adv. Eng. Mater. 18 (2016) 463–475.
- [6] E.O. Olakanmi, R.F. Cochrane, K.W. Dalgarno, A review on selective laser sintering/melting (SLS/SLM) of aluminium alloy powders: Processing, microstructure, and properties, Prog. Mater. Sci. 74 (2015) 401–477.
- [7] T.M. Yue, Y.P. Su, Laser multi-layer cladding of Zr65Al7.5Ni 10Cu17.5 amorphous alloy on magnesium substrates, J. Mater. Sci. 42 (2007) 6153–6160.
- [8] A. Ericsson, V. Pacheco, M. Sahlberg, J. Lindwall, H. Hallberg, M. Fisk, Transient nucleation in selective laser melting of Zr-based bulk metallic glass. Materials & Design. 195 (2020): 108958.
- [9] S. Hocine, H. Van Swygenhoven, S. Van Petegem, C. Sin Ting Chang, T. Maimaitiyili, G. Tinti, D. Ferreira Sanchez, D. Grolimund, N. Casati, Operando X-ray diffraction during laser 3D printing. Materials Today. 34 (2020): 30-40.
- [10] S. Hocine, S. Van Petegem, U. Frommherz, G. Tinti, N. Casati, D. Grolimund, H. Van Swygenhoven. A miniaturized selective laser melting device for operando X-ray diffraction studies. Additive Manufacturing (2020): 101194.

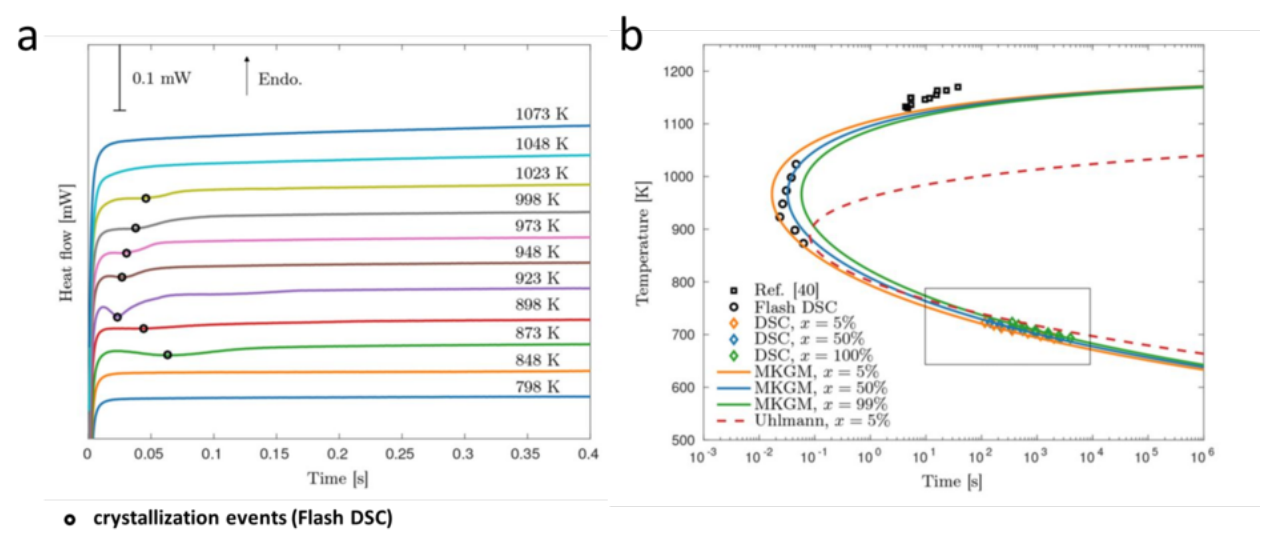


Figure 1:
a) Flash DSC scans of a Zr-based BMG and b) calculated TTT diagram at different crystalline volume fractions [8]

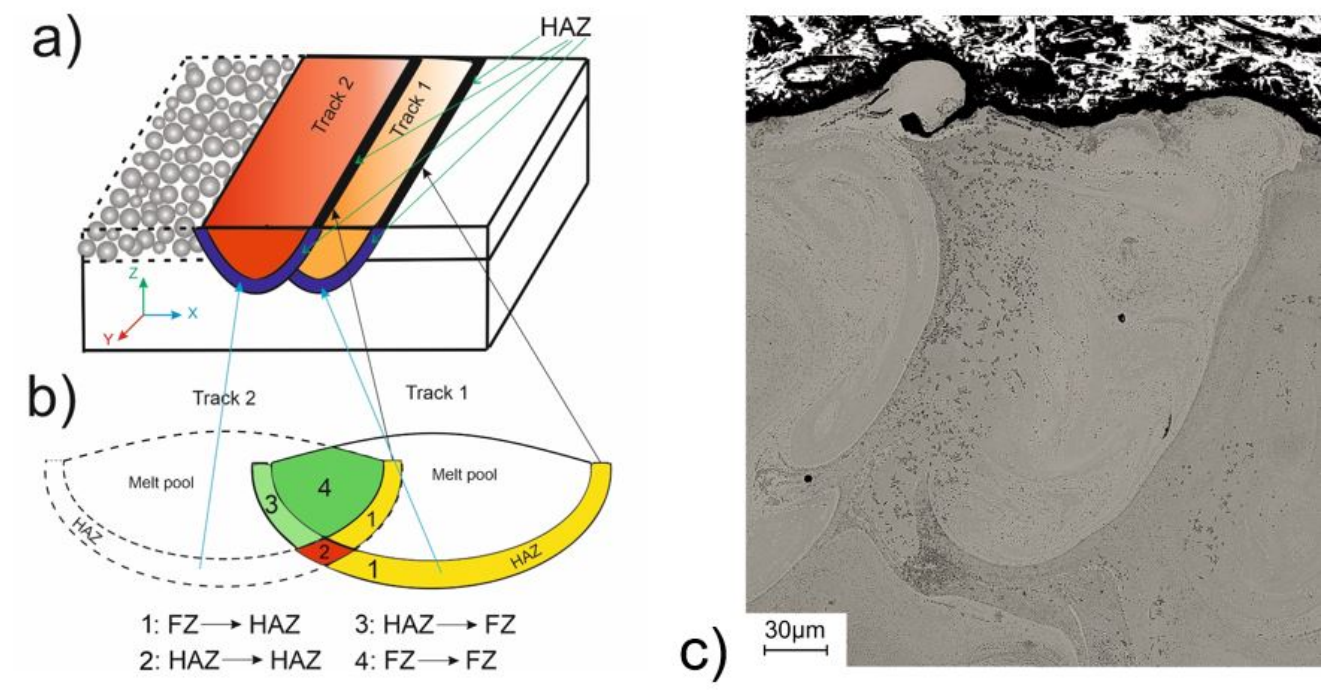


Figure 2:
a) and b) Schematic of the fused zone FZ and heat-affected zone HAZ during SLM;
c) Micrograph showing that crystallization occurs preferentially in the HAZ

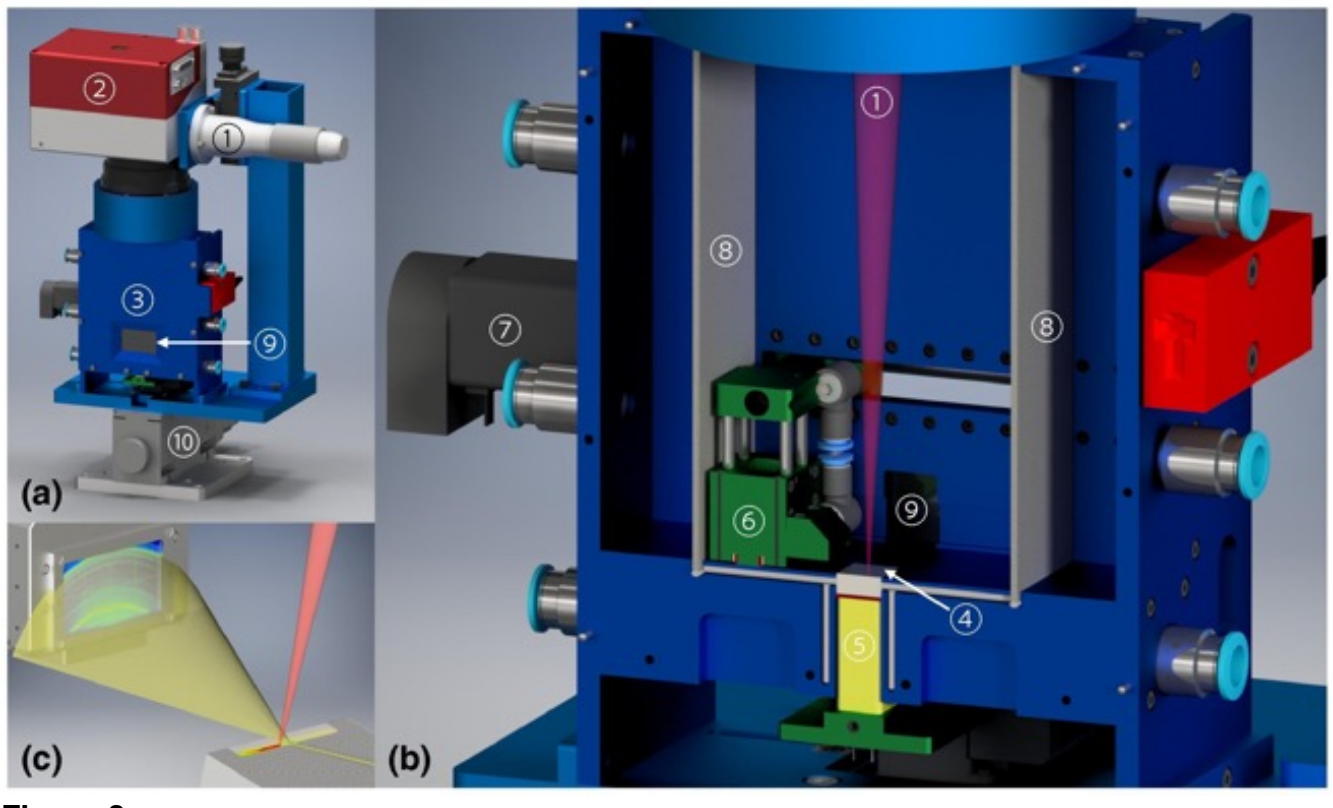


Figure 3: Schematic of the miniaturized SLM device. For more details, see [9]

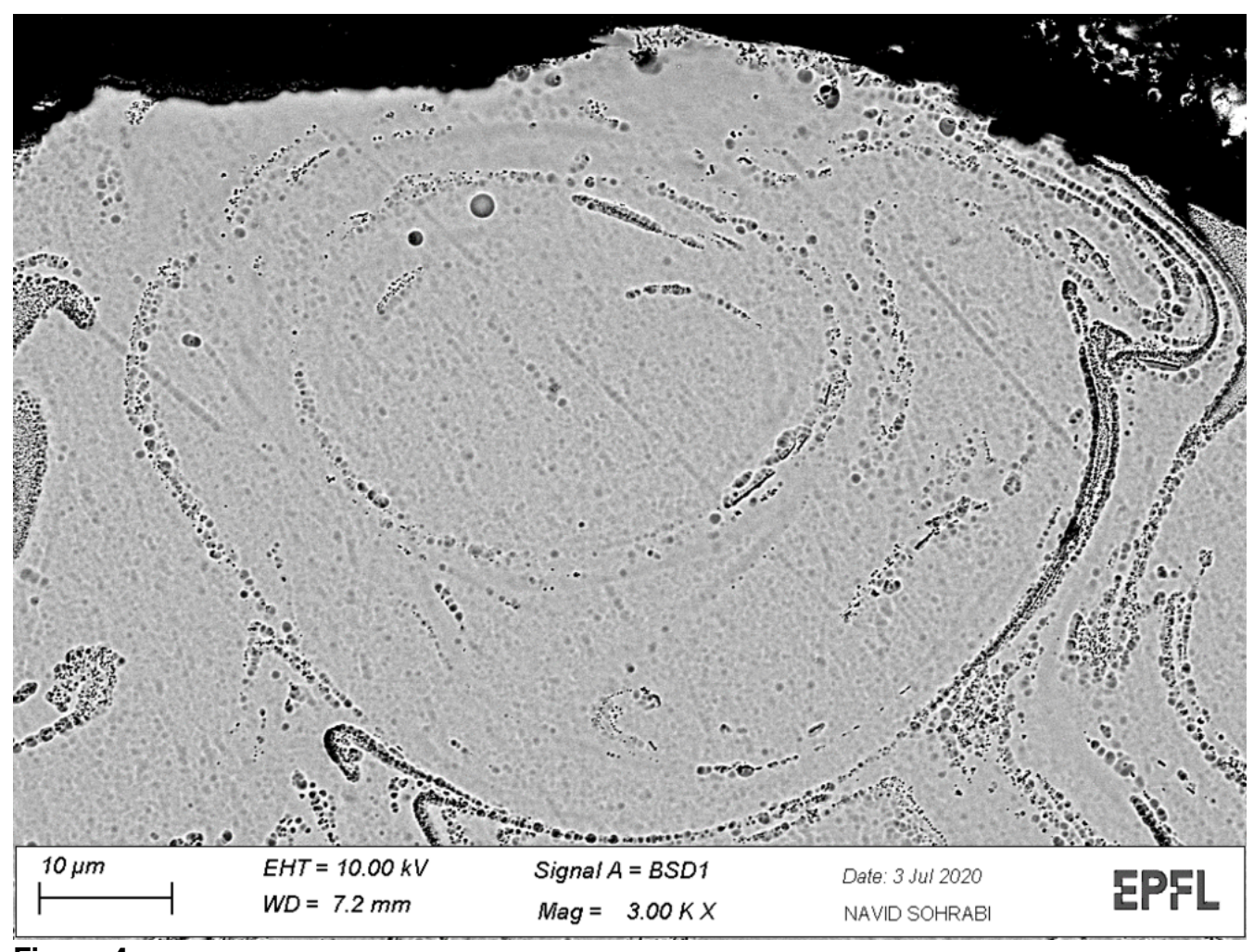


Figure 4:
SEM micrograph of nanocrystals in the HAZ and melt pool of a 2x2x0.05mm Zr-BMG foil

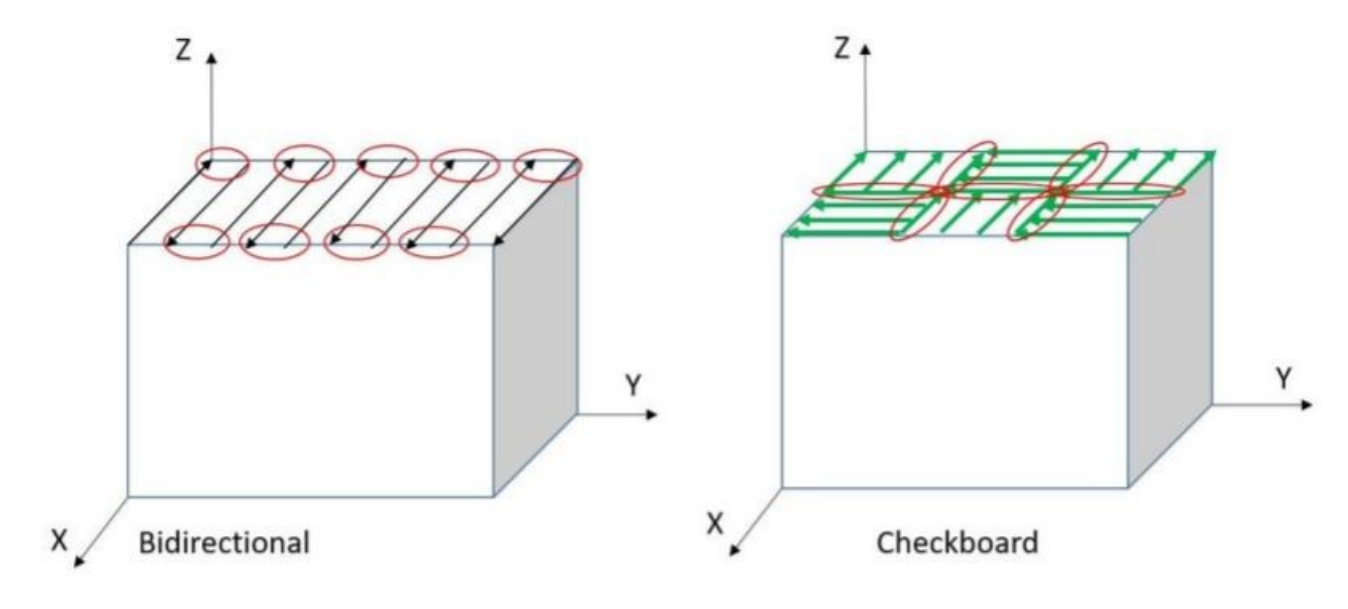


Figure 5: Effect of the scanning strategy on local heat accumulation (red circles)

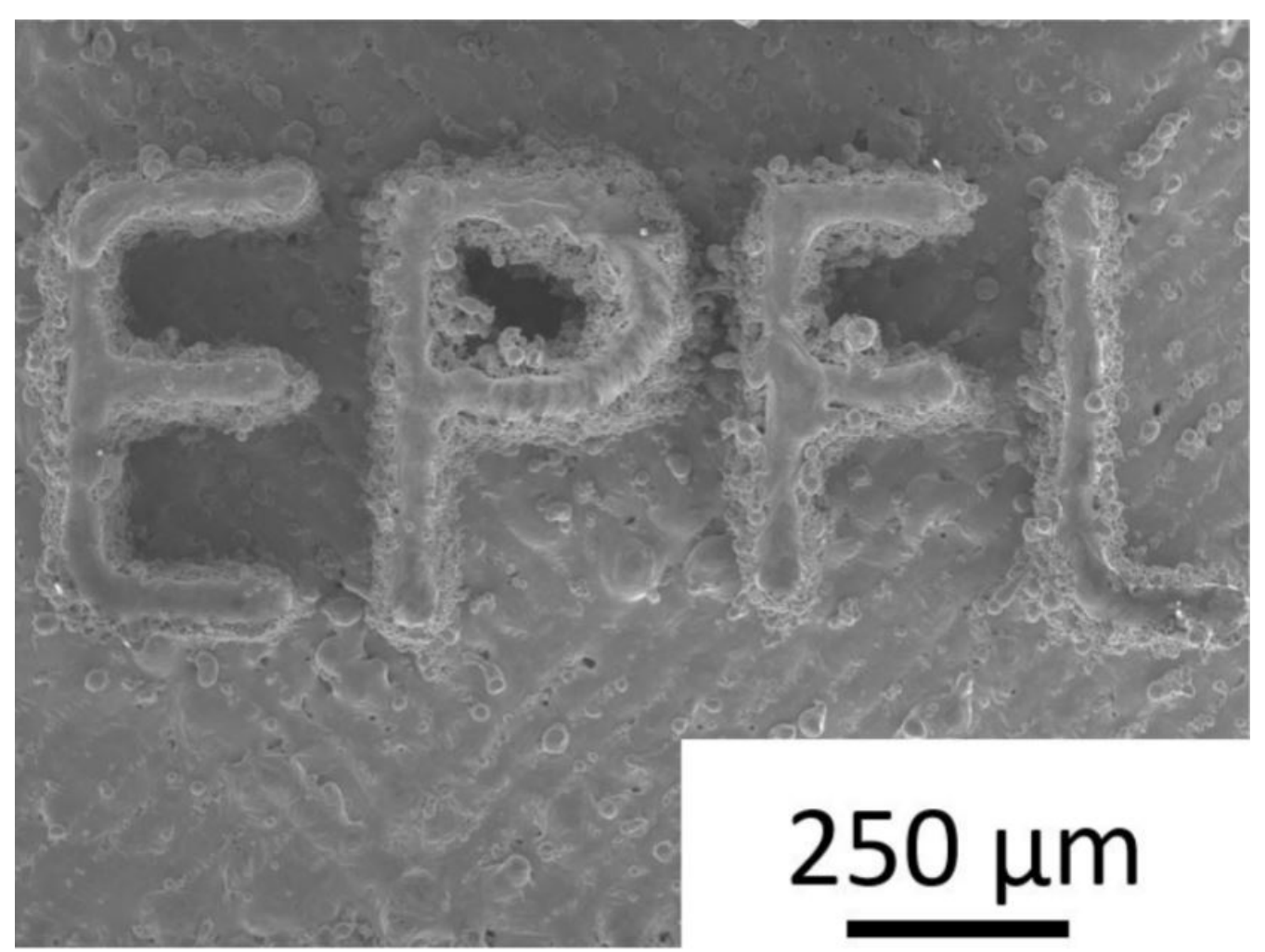


Figure 6:
Top-view of a thin wall Zr-based BMG